Journal of Materials Chemistry A

Accepted Manuscript

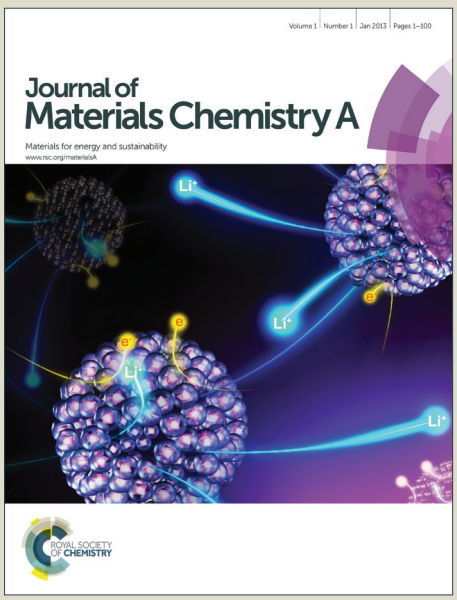

ROYAL SOCIETY OF CHEMISTRY

www.rsc.org/materialsA

Journal of Materials Chemistry A

Dynamic Article Links ►

Cite this: DOI: 10.1039/c0xx00000x

www.rsc.org/xxxxxx

PAPER

De novo assembly of mesoporous beta zeolite with intracrystalline channels and its catalytic performance for biodiesel production

Qiangqiang Zhang[a],Weixing Ming[a], Jinghong Ma [a]*, Jilong Zhang[a], Peng Wang[a], and Ruifeng Li [a]*

Received (in XXX, XXX) Xth XXXXXXXXX 20XX, Accepted Xth XXXXXXXXX 20XX

DOI: 10.1039/b000000x

Mesoporous beta zeolite was hydrothermally prepared directly using silanizing silica without any mesoporus templates by the bond-blocking principle. Si-C bond-blocking arose in the crystalline growth. The crystallization consumed more than 10 days and the material has fairly stable structure, even to be processed until 32 days later in the hydrothermal system. The characterization of XRD, N_2-adsorption/desorption, and TEM/SEM on the materials indicated that the beta zeolite is truly a spongelike mesoporous zeolite with BEA topology structure, which is consisted of the self-sustaining macroscopic zeolitic aggregates assembled from nanosized crystalline domains of zeolite beta with intracrystalline mesopores. The mesoporous beta zeolite presented extremely large external surface area and adjusting mesoporosity. Compared to conventional beta zeolite, FTIR results of pyridine (Py) and 2, 6-ditertbutylpyridine (DTBPy) demonstrated an increase of Lewis-site contribution and a large improvement of accessibility of bulky molecules in the mesoporous beta zeolite. Finally the mesoporous beta zeolite showed a significant activity in transesterification reaction of triolein to get methyl oleate (biodiesel) because of the accessibility increase and the diffusion-limitation reduction of large lipids to acid sites in the H-beta zeolite framework.

1. Introduction

Zeolite beta, one of the most important zeolitic materials in chemically and petrochemically industrial applications, has been shown to be a very active catalyst for many hydrocarbon reactions owing to its large window diameter in combination with strong acidic sites. The channel system of zeolite beta has three-dimensional architecture composed of the intersecting 12-ring channels with pore diameters of 0.55 × 0.55 nm and 0.76 × 0.64 nm, which are similar to other large-pore molecular sieves such as FAU and EMT zeolites. Even so, similar to other microporous zeolites having crystal sizes in the micrometer range, the conventional zeolite beta suffers from strong steric and diffusion limitations, which has led to an under-utilization of the potential of zeolites as catalysts in a number of catalytic reactions involving transformations with the participation of large compounds. It is well known that both reducing the crystal size of zeolite to less than 100 nm and creating additional porosity (hierarchical zeolites) in crystal of zeolite are effective strategies for increasing the accessibility of active sites and the rate of intracrystalline diffusion due to the increase of outer part of the crystalline framework and the reduction of the length of the diffusion pathway of reactants and products in the zeolite phase. Several review articles [1-5] have focused on this topic to survey the different strategies creating additional intra- or inter-crystalline mesoporosity in addition to the inherent microporosity of zeolites, which involved using the solid template, the soft template in the form of surfactants or polymers, or the post-treatment routes to generate intracrystalline mesopores and nanocrystal assembly routes to generate intercrystalline mesopores. Recently, our research group has synthesized successfully the zeolite LTA with the intracrystalline mesopores [6] and ZSM-5 zeolite microphere composed of nanocrystals with intracrystalline mesopores [7] in a one-step process by bond-blocking action during the crystal growth, in which the mesoporosity could be variable through adjusting the silanizing degree of surface on silica. The synthesis approach expanded a new idea to prepare the hierarchical mesoporous zeolites.

Recent publications documented the synthesis of beta zeolite with secondary pores. Xiao et al. used a hydrophilic cationic polymer, polydiallyldimethylammonium chloride (PDADMAC), to template intracrystal mesoporosity in single zeolite beta crystals with a disordered hierarchy of mesopores that ranged between 5 and 40 nm [8]; soon afterwards, stable zeolite beta particles with a high external surface area and large mesopore volume were fabricated from the self-assembly of zeolite beta nanocrystals with the cationic polymer PDADMAC [9]. Bein et al. prepared also the nanozeolite beta aggregates with secondary pores of tunable sizes by the flocculating action of a cationic polymer polydiallyldimethylammonium chloride (PDDA), that is, upon the addition of polymer, the nanoparticles were flocculated into self-sustaining, easily retrievable mesoporous aggregates in a one-step procedure, showing interparticle pores with very high mesopore volumes and surface areas[10]; furthermore, they reported an effective synthesis procedure for hierarchical zeolite beta that affords mesopores through controlled intergrowth of

nanosized crystallites into an open network without using a second porogen [11]. The preparations of hierarchical zeolites beta from packing of the nanozeolite produced in a multiple step procedure of evaporation, dilution, pH-adjustment, crystallization and subsequent centrifugation that result in mesoporous materials were reported by Petushkov [12]. Serrano and coworkers prepared a hierarchical zeolite beta material by hydrothermally treating zeolite beta nanocrystals by the functionalizing of organosilanes. The organic moieties provided mesopore spacing among the zeolite crystals [13]. Zhu et al. have achieved a method for the synthesis of intracrystal mesoporous zeolites with BEA and MEL topology by using polyvinyl butyral (PVB) as the mesopore directing agent [14]. Recently, the group of Ryoo [15] and Liu [16] reported respectively the synthesis of zeolites beta with a mesopore-micropore hierarchy through the dual-porogenic surfactant-driven synthesis route. In the process, the surfactants played a dual-functional role, that is, the mesopores are generated by surfactant aggregates, whereas the crystalline microporous zeolite frameworks are generated by the multiple quaternary ammonium groups. The mesoporous zeolites improved substantially the catalytic activities for various organic reactions involving bulky molecules compared with conventional zeolites. However, the direct assembling of mesoporous BEA zeolite is difficult using the existing techniques because of the connectivity of tetrahedra in both main polymorphs resulting in two straight channels and another one oscillating with windows (ca. 0.7 nm in diameter) composed of 12 T-atoms. The corresponding work has not been reported. In this contribution we attempt to explore an ordinary synthesis method of mesoporous zeolite beta using silanizing silica by bond-blocking principle. The mesoporous zeolitic material is employed to prepare biodiesel by the transesterification reaction of vegetable oils.

Zeolites are promising for acid-catalyzed transesterification reactions because of the diversity in their structures and Si-to-Al ratios, and they are enduring for high free fatty acid (FFA) concentrations of low-cost feedstocks [17], but the conventional zeolites still suffer, with lower conversion efficiency as a catalyst in biodiesel production from transesterification of oils due to the limitation of the accessibility of active sites to the reactants [18]. It is, therefore, imperative to develop mesoporous zeolites with high catalytical efficiency for the production of biodiesel.

This paper presents the result of the construction of hierarchically organized zeolite beta synthesized by employing organfunctioned fumed silica as silica source. XRD, N_2 adsorption/desorption, TEM/SEM were used to characterize the structure, texture and appearance of the resulted materials, and the infrared spectroscopy of adsorbed pyridine and di-tert-butylpyridine was used for investigating the total acidity and accessibility of acid sites in the corresponding samples. Moreover, the catalytic capability of the mesoporous zeolite beta in the transesterification of vegetable oil, of which the dominant component is the triglyceride form of oleic acid (C18:1), triolein, in excess methanol for biodiesel production has been demonstrated.

Experimental Section

Synthesis of the mesoporous structured zeolite beta

Synthesis of the mesoporous structured beta zeolite was carried out by employing organfunctioned nano-silica as silica source according to the similar procedures previously published by our research group [6, 7]. Fumed silica (Degussa, Aerosil 200) was firstly functionalized by organosilane PHAPTMS (phenylaminopropyl-trimethoxysilane, AR, Aldrich) at the molar ratio: SiO_2: $60H_2O$: xPHAPTMS: $6CH_3OH$, where x is from 0 to 0.2. Next, beta zeolite samples were prepared from a mixture with the following molar composition: Al_2O_3： 38 SiO_2： 1.5 Na_2O： 10 TEAOH： 532 H_2O. In a typical synthesis experiment, tetraethylammonium hydroxide (TEAOH, 25% aqueous solution), deionized water and sodium aluminate (AR) were mixed together and stirred until sodium aluminate was completely dissolved. Then, the desired amount of organfunctioned silica was added to the solution under stirring at room temperature to obtain a homogeneous gel mixture. The resultant mixture was subsequently transferred into a Teflon-lined stainless steel autoclave and heated at 413 K for 4-32 days. After crystallization, the collected precipitate was filtered, dried in air, and calcined at 823K to remove the microporous template. In a series of sample preparations, the molar ratios of PHAPTMS/SiO_2 were 0.075 and 0.15. The materials obtained were denoted as MBeta-1 and MBeta-2, respectively. A reference sample (denoted as Beta-0) was synthesized using unorganofunctionalized fumed silica under otherwise similar conditions.

The NH_4^+ form of samples was prepared by ion exchange for three times, at 353 K with 0.5 mol/L NH_4NO_3 solution for 4 h each time, and then washed with deionized water. The protonic form was then obtained by calcining the NH_4^+-zeolite at 823 K for 5 h.

Characterization of the mesoporous structured zeolite beta

Powder X-ray diffraction (XRD) patterns were obtained on a Shimadzu XRD-6000 diffractometer equipped with Ni filter using CuKα radiation with the step size and the counting time of 0.02° and 10 s, respectively. Nitrogen adsorption/desorption isotherms at 77 K were obtained in a Quantachrome NOVA 1200e. Prior to the analysis, the samples were outgassed at 613 K under vacuum for 5 h. The apparent surface area was obtained by the BET equation in the range between p/p_0 = 0.02-0.15, whereas the external surface area and micropore volume were calculated by the t-plots in the range between 0.12 and 0.4 p/p_0 (de Boer). The total pore volume was evaluated at p/p_0 = 0.99. The mesopore volume (V_{meso}) was calculated from the difference between the V_{tot} and V_{micro}. Pore size calculations were performed with the DFT method on the adsorption branch using nitrogen on silica, cylindrical pore NLDFT model. Field emission scanning electron microscope (SEM) images were obtained in a JEOL JSM-6700F. Transmission electron microscope (TEM) images were obtained in a JEOL JEM-1011. The samples were dispersed in ethanol and deposited on a holey carbon film supported on a Cu grid. Zeolite powder was immersed in ethanol and sonicated for about 30 min, and one to two drops was spread on the copper grids covered with holey carbon. For FTIR spectra of framework vibration as well pyridine (Py) and 2,6-ditertbutylpyridine(DTBPy) adsorption, the measurements are performed on a Shimadzu IRAffinity-1 spectrometer equipped with a vacuum cell. Infrared spectra of samples in the form of KBr pellets were recorded at the room temperature. Adsorption of

pyridine (Py) and 2, 6-di-tert-butylpyridine (DTBPy) was conducted on the outgassed samples at 423K, prior to the measurements, the catalysts were pressed in self-supporting discs and activated in the IR cell attached to a vacuum line at 723 K for 4 h. High resolution ^{29}Si MAS-NMR and ^{27}Al MAS-NMR spectra of the samples were recorded using a Varian UNION INOVA 300M spectrometer.

Transesterification Reaction

Transesterification of vegetable oils in excess methanol was carried out in a batch stirred reactor equipped with water-cooled condenser, which was placed in a constant-temperature oil bath over a magnetic stirrer. The predetermined amounts of catalysts, the commercial edible grade vegetable oil (an expired peanut oil was used), and methanol were sealed into the reactor. The transesterification is carried out at a weight ratio between methanol and oil of 15 in an initial feed, a weight ratio between catalyst and oil of 0.02, and reaction temperature at 423K. The reactor was sealed and stirred as it was heated to the temperature set-point. As the reactor heats up to the set-point, time zero (t=0) is selected as the moment when the set-point is reached. After reaching a preset reaction time, the reaction mixture was quickly filtered to separate solid catalyst. Methanol was then removed by a rotary evaporator, so glycerol can be separated by gravity filtration. The gas chromatograph equipped with a flame ionization detector and an Agilent-DB-5ht capillary separation column (15m×0.25m×0.25μm) was applied to quantify the glycerides and methyl fatty esters (biodiesel). Nitrogen was used as the carrier gas at a constant flow rate of 12 ml/min. The column oven temperature was programmed from 343 to 463 K (at the rate of 15 K/min) and then raised to 533 K at 7 K/min and to 653 K at 30 K/min and maintained at this temperature for 6 min. The analytics of the reaction mixture and the retention times of the products were supplied in the *supplementary information section*.

Results and discussion

The X-ray powder diffraction (XRD) patterns of Beta-0, MBeta-1 and MBeta-2 samples are shown in Figure 1. The diffraction peaks located at around 7.8 and 22.4 are indexed to the characteristic diffraction peaks of BEA topology structure, and no indication of impurities or amorphous unreacted silica was observed in the XRD patterns of all samples. Compared to Beta-0, Mbeta -1 and -2 samples exhibit broader reflections, indicating

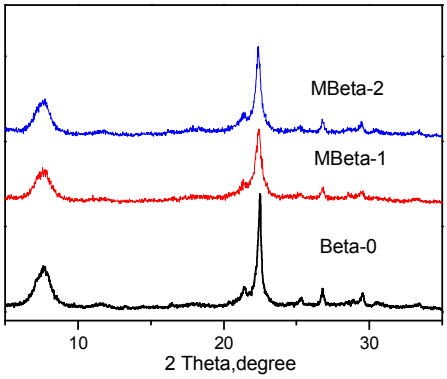

Fig.1 XRD patterns of Beta-0, MBeta-1 and MBeta-2 samples (Crystallization time 16 days)

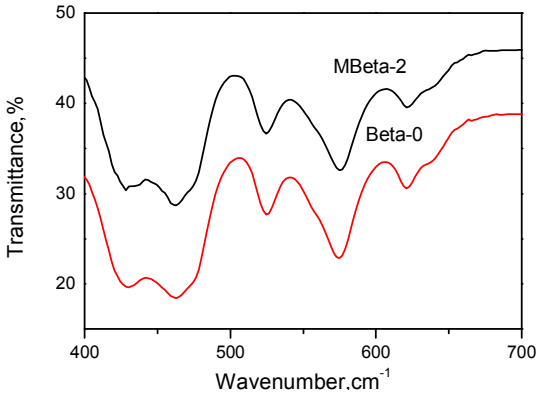

Fig.2 FT-IR framework spectra of Beta-0 and MBeta-2 samples

the presence of small domains. Another evidence for the structure of the zeolite beta is provided by the distinct absorptions at 575 and 525 cm^{-1} detected in the FT-IR framework spectra of the representative Beta-0 and MBeta-2 samples (Figure 2), which are attributed to the five- and six-membered rings of T–O–T (T= Si or Al) in the structure of Beta zeolite[19]. The results of XRD and IR prove the feasibility of synthesizing beta zeolite by using the organfunctioned nano-silica as the precursor. Although the crystallization consumes 16 days and more (crystallization curves of the beta zeolite were listed in Figure S1), a real mesoporous

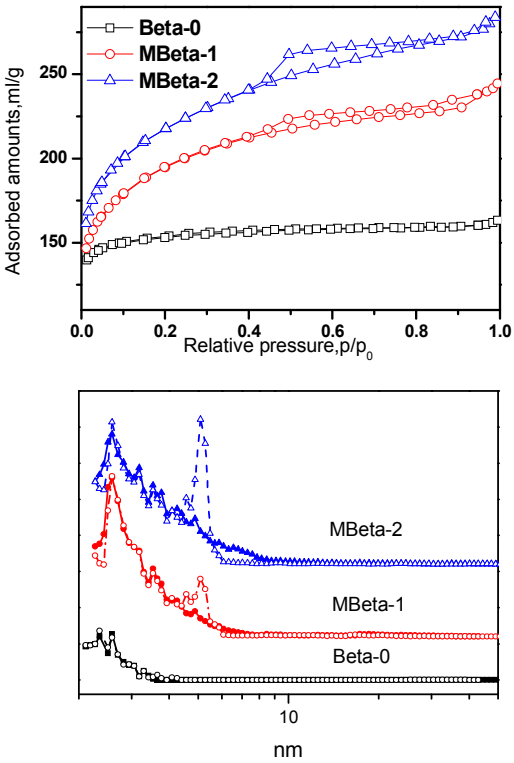

Fig. 3 N_2 adsorption/desorption isotherms at 77K of Beta-0, MBeta-1 and MBeta-2 samples (above) and corresponding NLDFT pore size analysis derived from the adsorption(solid lines) and desorption(open lines) branch (below)

Table 1 Pore structure parameters of Beta-0, MBeta-1 and MBeta-2 from N_2 adsorption isotherms

Samples	S_{BET} (m^2/g)	S_{MIC}(m^2/g)	S_{EXT}(m^2/g)	V_{MIC}(cm^3/g)	V_{MESO}(cm^3/g)	HF*
Beta-0	649	623	27	0.24	0.03	0.04
MBeta-1	713	461	252	0.16	0.21	0.15
MBeta-2	801	472	329	0.17	0.25	0.17

* HF is the hierarchical factor, defined as $(V_{mic}/V_{total})\times(S_{EXT}/S_{BET})$[21]

beta zeolite with high crystalline degree has been prepared.

N_2 adsorption/desorption isotherms at 77K revealed the difference of the pore structures between the reference sample Beta-0 and MBeta-1, -2 samples derived from the silylated SiO_2. As shown in Figure 3a, Beta-0 presents a typical type I isotherm, reflecting its intrinsic microporous structure; the MBeta-1, -2 samples show the gradual but continuesly rising curves after a steep uptake from micropore filling in the low relative pressure region of $p/p_0 < 0.01$, and a hysteresis from $p/p_0 = 0.45$ to 1, which are the results of N_2 adsorption and capillary condension in the mesopores. These analyses confirm co-existence of micropores and mesopores in MBeta-1 and -2 samples. The mesopore size distributions estimated from the adsorption branch of the isotherms using NLDFT method exhibit the pore size distribution of mesopore diameters between 2 and 10 nm and majority of mesopores are in the range of 2-3 nm (Figure 3b). Moreover, it is noticed that the pore size distribution by applying the NLDFT adsorption branch kernel on the adsorption isotherm is nearly identical to that from the equilibrium kernel on the desorption branch with the exception of the PSD artifact obtained from the section of desorption branch with the characteristic step-down in the desorption isotherm, showing that the hysteretic originates solely from delayed nitrogen condensation [20]. It seems that the pore blocking or percolation effects are not present, and the mesopores are well defined cylindrical continuous pores to be open to the external surface of the crystals, which would be very important to the improve accessibility of the mesoporous zeolite beta [11]. Table 1 listed the quantitative analysis of the pore structure based on N_2 adsorption/desorption isotherms. As compared with conventional microporous Beta-0 (reference sample), either MBeta-1 or MBeta-2 sample possesses not only a larger BET surface area but also a much larger mesopore volume and external surface area, especially MBeta-2 prepared by using the SiO_2 with higher surface silanizing degree. Although the end of the isotherms of the two mesoporous zeolite materials slightly sideways upward as p/p_0 approaches 1, the maroporous (between 100 and 200 nm) proportion is very small. Tha fact has been verified by a mercury method that the pore volum of the MBeta-2 is 0.02 cm^3/g （Figure S2）. Thus results in the mesoporous beta zeolites having high HF factors. These results validate the generation of mesoporosity from the intra-crystal of zeolites or the inter-crystal of zeolite aggregates assembled by small size of the zeolite particles (also see the following results of SEM and TEM).

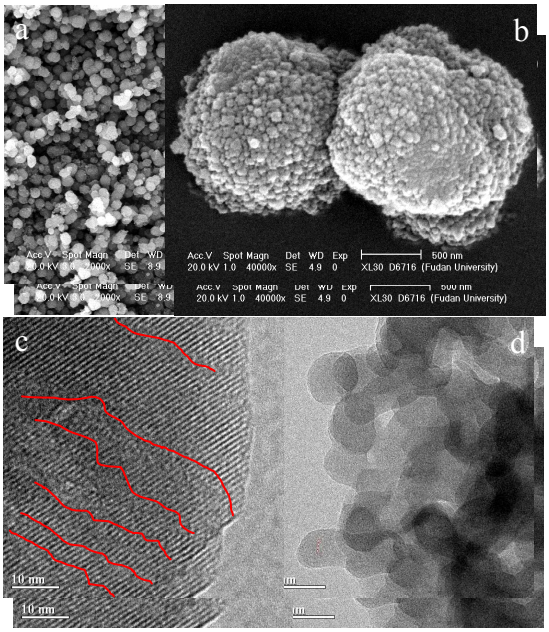

Fig. 4 SEM (a, b) and TEM (c, d) images of MBeta-2

Fig. 4 SEM (a, b) and TEM (c, d) images of MBeta-2

The SEM images in Figures 4(a, b) demonstrated the detailed information on the morphology of the MBeta-2 sample. The SEM images at the low magnification show that the particles of the beta zeolite are relatively uniform. The high-magnification SEM images illustrate that the beta zeolite particles are in the nearly spherical shape with a diameter of about 1.5-2 μm, and the surfaces rough. The micrometer-sized particles are found to be particle aggregating with the nanosized crystallites of around 50-100 nm, and there are intercrystal mesoporosity attributed to the voids between the nanosized units. TEM is used to investigate the internal structure of the materials. Figure 4(c, d) exposed the representative high-resolution TEM images of the mesoporous

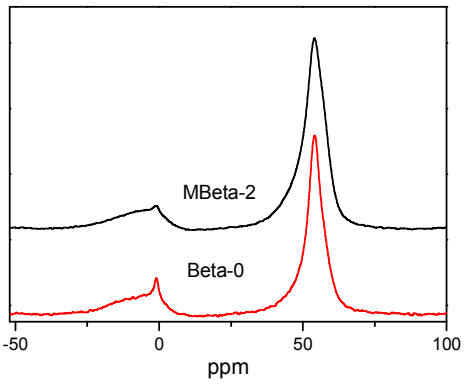

Fig. 5 ^{27}Al MAS NMR spectra of Beta-0 and MBeta-2 samples

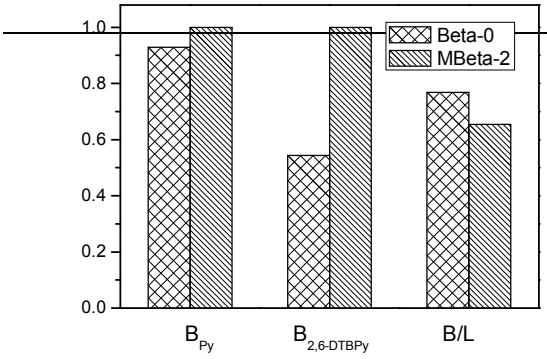

Fig. 6 Relative contents of Brønsted sites accessible for Py and DTBPy and B/L in Beta-0 and MBeta-2 samples

beta zeolite, which is taken from the edge of a selected crystal particle and the lattice fringes can be clearly distinguished. The ordered micropores and channels which have arisen from the crystalline structure are well arranged in the crystal, revealing the high crystallinity of this sample. On the other hand, the irregular mesopores are randomly distributed throughout the crystal. These mesopores and micropores are located in the same matrix, constructing a pore system with a hierarchical architecture (Accessorial TEM images were offered in Figure S3).

According to the characterization above of N_2 adsorption, SEM and TEM, the synthesized beta zeolite material by using the organfunctioned nano-silica precursor possesses two additional pores in the meso-scale, that is, the intercrystal and intracrystal mesopores, resulting in the extremely large total and external surface areas in the zeolite materials. The hierarchically structured zeolite can provide a large number of external active sites and a short diffusion route for the guest molecules, which are important for any of the catalysis involving bulky molecules.

The structural configuration of Al atoms in the conventional microporous Beta-0 and the mesoporous MBeta-2 samples was investigated by ^{27}Al MAS NMR spectroscopy (Figure 5), which is powerful in identifying the environmental conditions of the zeolite samples. Clearly, both the Beta-0 and MBeta-2 samples exhibit two resonance peaks at a chemical shift of 54 ppm and -1 ppm respectively, corresponding to the tetrahedrally coordinated framework Al and the octahedrally coordinated nonframework Al, which demonstrates that the most of Al is incorporated in the framework of the MBeta-2 as Beta-0, but it can be observed that the peak shape of the tetrahedrally coordinated aluminium is broadened, which indicate that the homogeneity of Al in the atoms environment of the MBeta-2 was decreased in comparison with that of Beta-0, which is derived from the increase of external surface area of the zeolite [16].

Infrared spectroscopy of adsorbed pyridine (Py) and di-tert-butylpyridine (DTBPy) were studied in order to realise the total acidity and accessible acid sites within the mesoporous beta zeolite materials. Figure 6 illustrated the relative amounts of Brønsted (B_{py}) and Lewis (L_{py}) acid sites based on the pyridine adsorption from the bands at 1545 cm^{-1} and 1454 cm^{-1}, as well as that of the Brønsted sites (B_{DTBPy}) based on the DTBPy adsorption from the bands at 1615 cm^{-1} in the H-Beta-0 and H-MBeta-2 samples. The Si/Al ratios of Beta-0 and MBeta-2 are respectively 17 and 11, therefore it is plausible that the amount of total acid sites of H-MBeta-2 is higher than that of Beta-0, although the increase of L-site contents is much more notable than that of B-sites, and the ratio of B/L decreases. The results are most likely due to the destruction of some Si–O–Si and Si–O–Al bonds and to the formation of additional AlOH groups. But then, the acid strength of H-Beta-0 is higher than that of H-MBeta-2 according to the NH_3-TPD results (Figure S4). Furthermore, it is amazing that all the B-sites in H-MBeta-2 are nearly accessible by DTBPy. However, only 50% B-sites in H-Beta-0 can be reachable. Since pyridine with a smaller size (0.58 nm) can reach almost all acid sites in beta zeolite with the pore dimension (0.76 nm x 0.64 nm) [19], it was logically assumed to probe Brønsted and Lewis acid sites in the zeolite material. And yet the molecular size of DTBPy is about 0.79 nm and very close to the dimension of pores in zeolite beta, theoretically the DTBPy molecules transfer supposedly into the micropores of zeolite beta, the diffusion inside the pores must be very limited, and therefore not all the sites inside the crystals could be accessible by DTBPy as a probe molecule accessible Brønsted sites in the samples. The creation of the mesopores in the zeolitic crystals and the increase of external surface area of zeolite particles both facilitate the diffusion of bulky molecules and improve the accessibility of the Brønsted acid sites by the corresponding molecules.

The introduction of mesoporous structure in zeolite with strong acidity can be remarkablly beneficial to catalytic reactions involving larger reactant molecules, since the diffusion constraint and/or adsorption of reactant molecules onto the strong acid sites are very important and sometimes crucial. Here, the catalytic activities of the mesoporous beta zeolite samples were studied by the transesterification reaction of triolein as a probe reaction. Triolein is a triglyceride with oleic acid carboxylic groups and each hydrocarbon chain consists of 18 carbon molecules and one double bond, therefore the transesterification of triolein is a typical reaction involving bulky reactant molecules and requiring strong acidity. The procedure involves the reaction of triolein with methanol in the presence of a catalyst to form fatty acid methyl esters (FAME, the chemical name of biodiesel) and glycerol. The reaction consists of three consecutive and reversible steps, that is, the conversion of triolein (TOL) to diolein (DIO),

Table 2. Conversion of triolein and products composition of Beta-0 and MBeta-2

Catalyst	Reaction time, h	TOL Conv. Wt %	Product composition, wt%			
			TOL	DIO	MONO	MEO
Beta-0	0	0	61.6	33.5	3.00	1.90
	3	6.44	63.3	21.4	5.20	4.10
	6	11.0	57.0	32.6	3.10	7.40
	27	16.6	54.8	26.5	10.3	8.40
MBeta-2	3	16.2	53.2	19.4	11.9	15.5
	6	95.4	3.20	7.60	24.2	71.3
	27	100				100

that of DIO to monoolein (MONO), and that of MONO to methyl oleate (MEO) and glycerol. As expected, H-MBeta-2 showed a much higher catalytic activity for transesterification reaction of triolein than those of conventional Beta-0 zeolite. The catalytic results were listed in Table 2. The feedstock composition was measured to contain 61.6 wt% triolein, 33.5 wt% diolein, and 3.0 wt% monoolein. The data indicates that the pure microporous H-Beta-0 catalyst has very low catalytic activity and poor effect on transesterification of triolein. The conversion of triolein to biodiesel reaches 6.44% after a transesterification reaction for 3 h, 11.0% after 6 h, and even only 16.6% even if after 27 h of the reaction and the MEO content in product is only 8.40%. In contrast, using the mesoporous H-MBeta-2 as the catalyst, the conversion of triolein to biodiesel has been greatly improved. The conversion of triolein reaches 15.5%, 71.3% and 100% respectively after 3 h, 6 h and 27 h of the transesterification reaction, respectively, and the MEO content in product is 71.3% and 100% in the corresponding period. The data can be reproduced in the experiment. Compared to H-Beta-0, H-MBeta-2 could significantly shorten the reaction time required to reach the same level of conversion. From the results above, it is known that the conventional zeolite beta is active catalyst for the transesterification of triolein, but has rather slow reaction rate due to the limitations of accessibility and diffusion for the lipids to penetrate to the internal active sites located inside the zeolite microporosity. By diffusion, triolein with dynamic diameter of 2.82 nm (Figure S5) is impossible to come into contact with the active acid sites on the inner pores of zeolite beta with microporous and but without mesoporous structures, or in other words, the beta zeolite has very low accessibility of active acid sites to the big molecules except the few exteral active sites of the zeolitic particles. The result is the beta zeolite has lower catalytic activity. Brito et al. once reported the lower conversion efficiency attained, which is near 26.6%, by using zeolite HY as the catalyst for transesterification of used vegetable oil in a continuous tubular reactor at a high temperature of 749 K [18]. Thus, it seems that an ideal solid acid catalyst for the transesterification of triolein should show an interconnected system of large pores to minimize diffusion problems of the molecules having long alkyl chains. For the mesoporous H-MBeta-2 sample, it presents a large external surface area together with interconnected mesoporous porosity, therefore, the accessibility and the diffusion of bulky lipid molecules to the active sites are improved greatly, and their ability to catalyze the transformations of bulky compounds is enhanced.

Conclusions

The hierarchical self-sustaining macroscopic beta zeolite aggregates assembled from the nanosized crystalline domains of zeolite with intracrystalline mesopores was successfully synthesized by employing organfunctioned nano-silica as silica source in a hydrothermal system. These materials retain their microporosity while simultaneously showing extremely high external surface area and mesoporous volume derived from the intracrystalline mesopore and the assembly of nanosized crystalline beta zeolite particles, and their mesoporosity might be adjusted through varying the silanizing degree of surface on silica. The creation of mesopores resulted in the increasing contribution of Lewis sites in the H-MBeta-2 sample due to the increase of contents of SiOH and AlOH groups from the external surface area and the improvement of their accessibility for the bulky probe molecules di-tertbutylpyridine. On the other hand, hierarchical H-MBeta-2 zeolite catalyst showed the much higher activity in the transesterification reaction of triolein to get methyl oleate than the conventional beta zeolite. The reason was attributed to the presence of a secondary mesoporosity in mesoporous beta zeolite, which increased the accessibility and reduced the diffusion limitations for bulky lipids molecules to reach the zeolitic acid active sites. Therefore, the hierarchically structured beta zeolite can be extended to be a promising candidate as a catalyst for many other acid-catalyzed reactions involving bulky molecules that could not enter the micropores of the conventional zeolites. Currently, further research is still under way in our laboratory.

Acknowledgements

This work was mainly supported by the National Nature Science Foundation of China (Grant No. 50872087).

References

1 S. Lopez-Orozco, A. Inayat, A. Schwab, T. Selvam and W. Schwieger, *Adv. Mat.*, 2011, 23(22-23), 2602.
2 R. Chal, C. G rardin, M. Bulut and S. van Donk, *ChemCatChem*, 2011, 3, 67.
3 D. P. Serrano, J. M. Escola and P. Pizarro, *Chem. Soc. Rev.*, 2013, 42(9), 4004.
4 L.Chen, X. Li, J.Rooke, Y.Zhang, X. Yang, Y. Tang, F. S. Xiao and B. L. Su, *J. Mater. Chem.*, 2012, 22, 17381.
5 K. Na, M. Choi and R. Ryoo, *Microporous Mesoporous Mater.*, 166 (2013) 3–19
6 Z. Xue, J. Ma, W. Hao, X. Bai, Y. Kang, J. Liu and R. Li, *J. Mater. Chem.*, 2012, 22(6), 2532.
7 Z. Xue, J. Ma, J. Zheng, T. Zhang, Y. Kang and R. Li, *Acta Mater.*, 2012, 60(16), 5712.
8 F. S. Xiao, L. F. Wang, C. Y. Yin, K. F. Lin, Y. Di, J. X. Li, R. R. Xu, D. S. Su, R. Schloegl, T. Yokoi and T. Tatsumi, *Angew. Chem.,* 2006, 118, 3162.
9 J. Song, L. Ren, C. Yin, Y. Ji, Z. Wu, J. Li and F. S. Xiao, *J. Phys.Chem. C*, 2008, 112, 8609.
10 K. Moeller, B. Yilmaz, U. Mueller and T. Bein, *Chem. Mater*., 2011, 23, 4301.
11 K. Moeller, B. Yilmaz, R. M. Jacubinas, U. Mueller and T. Bein, *J. Am. Chem. Soc.*, 2011, 133, 5284.
12 A. Petushkov, G. Merilis and S. C. Larsen, *Microporous Mesoporous Mater.*, 2011, 143, 97.
13 D.P. Serrano, J. Aguado, J. M. Escola, J. M. Rodriguez and A. Peral, *Chem. Mater.*, 2006, 18, 2462.
14 H. Zhu, Z. Liu, D. Kong, Y. Wang, and Z. Xie, *J. Phys. Chem. C*, 2008, 112, 17257.
15 K. Cho, K. Na, J. Kim, O. Terasaki and R. Ryoo, *Chem. Mater.*, 2012, 24, 2733.
16 B. Liu, Y.Tan, Y. Ren, C. Li, H. Xi and Y. Qian, *J. Mater. Chem.*, 2012, 22, 18631.
17 R. Jothiramalingam and M. K.Wang, Ind. Eng. Chem. Res., 2009, 48, 6162.

18 A. Brito, M. E. Borges and N. Otero, *Energy Fuels*, 2007, 21, 3280.
19 S. Mintova, V. Valtchev, T. Onfroy, C. Marichal, H. Knözinger and T. Bein, *Microporous Mesoporous Mater.*, 2006, 90, 237.
20 M. Thommes, *Chemie Ingenieur Technik*, 2010, 82(7), 1059.
21 J. Pérez-Ramírez, D. Verboekend, A. Bonilla and S. Abelló, *Adv. Funct. Mater.*, 2009, 19(24), 3972.

[a] *Key Lab of Coal Sci. & Tech. MOE, School of Chemistry and Chemical Engineering, Taiyuan University of Technology. Taiyuan 030024, CHINA. Fax/ Tel: +86 351 6010121; E-mail: rfli@tyut.edu.cn; majinghong@tyut.edu.cn*

† *Electronic supplementary information (ESI) available: Crystallization curves and TEM images of mesozeolitebeta zeolite.*